

Serpentinized peridotite-hosted uranium mineralization (U–Cr–Ni–Mo–REE–Fe–Mg) in Kudada–Turamdih area: A new environment of Metallogeny in Singhbhum shear zone, India

D. K. Sinha*, Shekhar Gupta, K. Nautiyal, V. R. Akhila, V. K. Shrivastava, A. K. Padhi and M. B. Verma

Atomic Minerals Directorate for Exploration and Research, Hyderabad 500 016, India

Recent exploration efforts in Kudada–Turamdih area has brought to light, for the first time, serpentinized-peridotite-hosted uranium mineralization (up to 0.188% U_3O_8) of polymetallic nature (U–Cr–Ni–Mo–REE–Fe–Mg) in the domain of Singhbhum Shear Zone (SSZ). The peridotite has been emplaced into the Iron Ore Group (IOG) and represents late phase activity in the IOG. Exploratory drilling has established substantial lateral (600 m) and downdip (1000 m) continuity of the mineralization. Subhedral to anhedral disseminated uraninite grains (10–600 μm) with cell dimensions of 5.4498 to 5.4650 Å suggest crystallization in meso to hypo-thermal range (300–500°C). Magnetite, chromite, molybdenite, cobaltite, nickeline, vaesite, cerussite, pyrite and chalcopyrite have also been identified in the REE enriched (Av. 1457 ppm) uraniferous peridotite. Presence of MgO (18–28%), Cr (295–3165 ppm), Ni (222–9530 ppm), Au (11–30 ppb), Pt (47–95 ppb) and As (15–755 ppm) suggests komatiitic parentage of host rock. Discovery of polymetallic mineralization in serpentinized peridotite, a hitherto unknown geological environment, opens up scope for further research and enhancement of uranium resources in the SSZ.

Keywords: Polymetallic, mineralization, serpentinized peridotite, Singhbhum Shear Zone, uranium.

THE Singhbhum Shear Zone (SSZ) is one of the most important polymetallic metallogenic provinces in India (Figure 1a). The SSZ hosts seven presently active uranium mines, some rich Cu deposits with by-products of Ni, Mo, Te, and Au, and many small apatite–magnetite ore bodies. The known uranium deposits and occurrences along the shear zone are hosted by volcano-sedimentary

rocks of the Singhbhum Group (SG), Dhanjori Group and to a lesser extent by Soda granite/feldspathic schist^{1,2}. Uraninite is the most abundant and ubiquitous uranium-bearing ore mineral in the deposits of the SSZ along with traces of brannerite, davidite, pitchblende, allanite, xenotime, autonite, torbernite and uranophane^{3–5}. Insignificant, minor uranium occurrences are also reported in metabasic and ultrabasic rocks (epidiorite/amphibolite schist), but in general they are not mineralized^{6,7}.

In the central part of the shear zone, exploration efforts in and around Turamdih uranium deposit have continued in two phases, i.e. 1950–1973 and 1982–1993. Production mining started in 2003 and is continuing till date. The present phase of exploration has been taken up in the vicinity of Turamdih from 2014 to enhance the life of the Turamdih mine by exploring adjoining areas. The Turamdih uranium deposit is hosted by the SG. During exploratory drilling in the SSZ, prominent quartz sericite schist was established as the footwall marker of the uranium lodes⁸. The depths of exploratory boreholes in Turamdih area were, therefore, constrained by this marker quartz sericite schist unit of the SG.

The recent phase of exploration was initiated with the above background to probe the base of the Iron Ore Group (IOG) through the SG, for quartz pebble conglomerate (QPC) type of uranium mineralization at a depth of more than 500 m. The boreholes have intercepted serpentinized peridotite with polymetallic (U–Cr–Ni–Mo–REE–Fe–Mg) nature intruded into the IOG. The mineralization intercepted in this unusual host rock was found to extend in deeper levels (up to 650 m) compared to the depths of mineralized lodes (300–350 m) explored during earlier phases of exploration in the SG. This article provides a report of polymetallic (U–Cr–Ni–Mo–REE–Fe–Mg) mineralization in serpentinized peridotite in the domain of the SSZ at deeper levels, but in the IOG.

*For correspondence. (e-mail: dksinha.amd@gov.in)

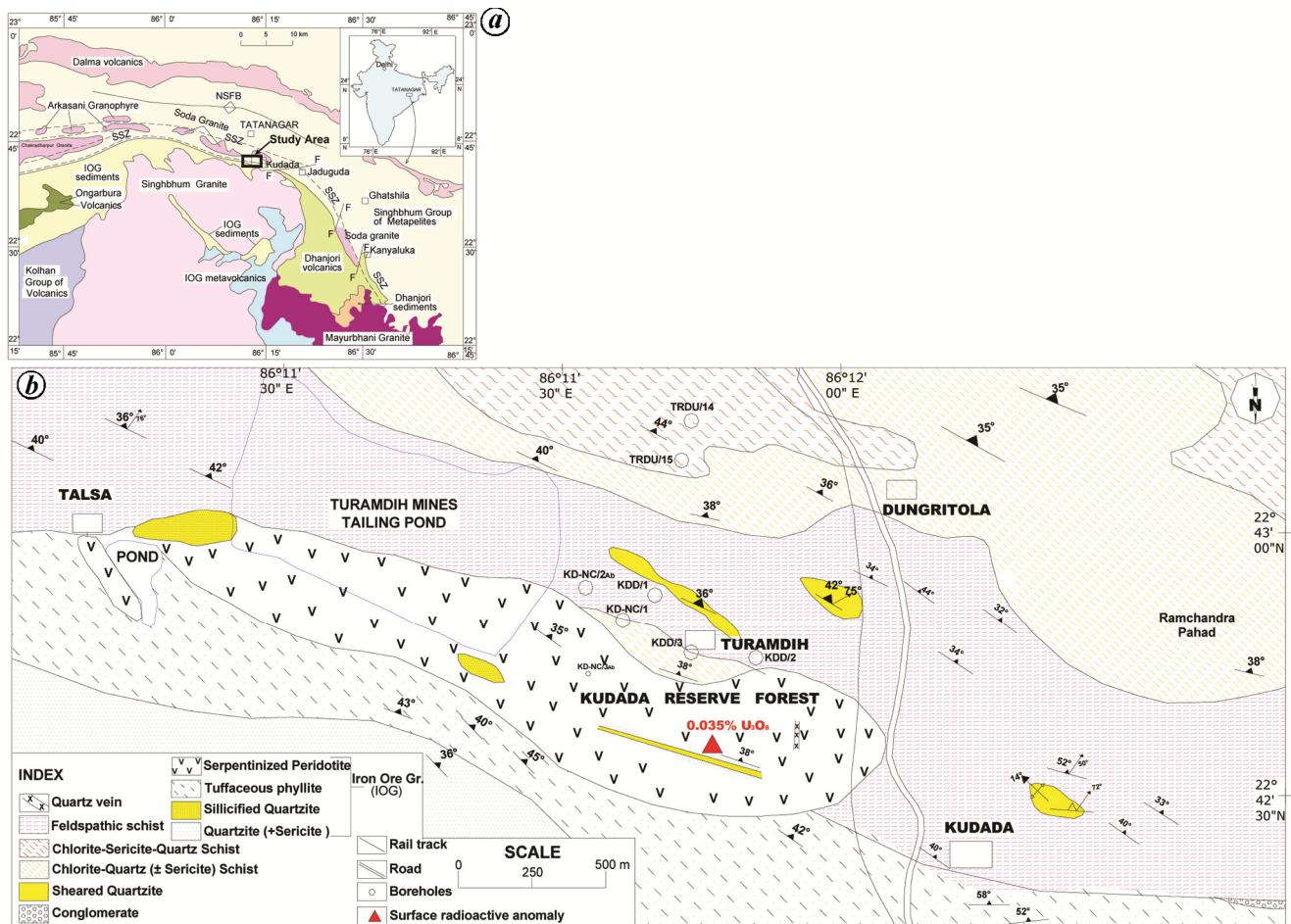


Figure 1. *a*, Regional geological map of Eastern Indian Shield around Singhbhum Shear Zone (SSZ) showing Kudada area (modified after Saha⁹). *b*, Geological map of Kudada–Turamdih–Nandup area, Jharkhand, India.

Regional geology

The Eastern Indian Shield mainly comprises Chotanagpur Granite–Gneiss Complex (CGGC) in the north, Singhbhum Craton in the south and E–W trending Proterozoic North Singhbhum Mobile Belt separating the two. The Singhbhum Craton is roughly oval-shaped, bounded by the arcuate-shaped SSZ in the north, the Sukinda thrust in the south, and Tertiary sediments of the Bengal Basin in the east. The ~200 km long, arcuate, intensely deformed SSZ borders the Archean cratonic nucleus in the south and the North Singhbhum Mobile Belt in the north (Figure 1 *a*)⁹. The Singhbhum Craton is a granite–greenstone terrain comprising large composite granite–tonalite batholith known as Singhbhum Granite Complex. Available geochronological data indicate that the nucleus of the craton formed between ~4.2 (ref. 10) and ~2.8 Ga (ref. 9). Subsequently, it experienced various phases of basin development and tectonism to acquire the present day litho-assemblage. The IOG rocks flank the Singhbhum Granite Complex on the eastern (Gorumahisani–Badampahar, the eastern belt), western (Noamundi–

Jamda–Koira, the western belt) and southern margins (Tomka–Daitari, the southern belt). The succession in these belts commences with a sandstone–conglomerate association at the base (QPC), followed by ferruginous shales, tuffs, ultramafic–mafic lavas (locally felsic) and the vast banded iron formation (BIF)^{11,12}. The North Singhbhum Belt is represented by (a) extensive siliciclastic rocks belonging to SG, and (b) intercalated late early–middle Proterozoic volcano-sedimentary rocks and mafic–ultramafic intrusions of the Dhanjori Group and Dalma volcanic belt. The SSZ transgresses the rocks of SG, Dhanjori Group and the IOG situated at the northern periphery of the Singhbhum Granite Complex^{12–14}.

Local geology

The area around Kudada and Turamdih exposes the IOG, SG and Singhbhum Granite Complex. SG contain schistose rocks with varying proportions of quartz, sericite and chlorite (\pm tourmaline, \pm apatite, \pm magnetite) and soda granite/feldspathic schist (Figure 1 *b*). Soda granite is

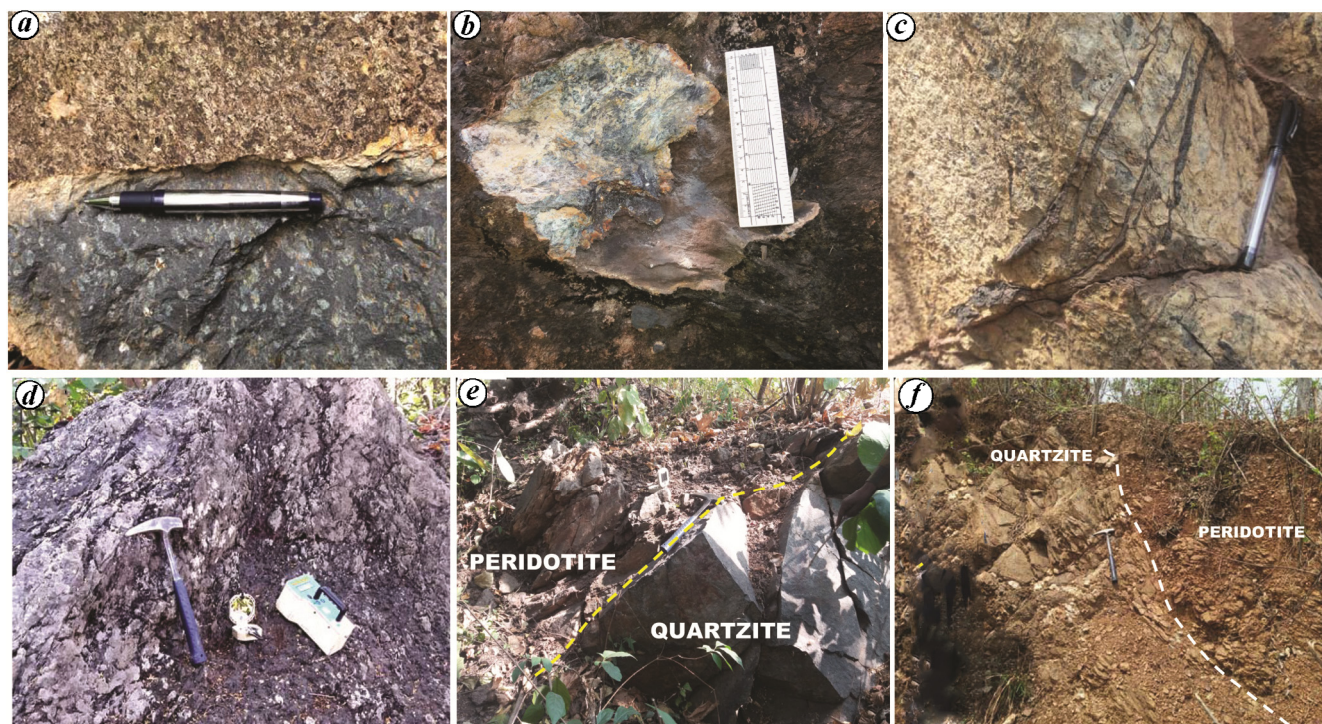


Figure 2. Field photographs showing the host rock in Kudada–Turamdih area. *a*, Altered relicts of olivine and pyroxenes in peridotite outcrop, Kudada area. *b*, Serpentine along broken faces of altered peridotite outcrop, Kudada area. *c*, Magnetite veins in serpentinized peridotite, Kudada area. *d*, Uraniferous serpentinized peridotite, Kudada area. *e* and *f*, Intrusive uraniferous peridotite in contact with IOG Quartzite, Turamdih area.

considered to be the product of Na-metasomatism by some authors^{15,16} and intrusive igneous rocks by some others¹. It has been dated ~2.2 and 1.6–1.4 Ga (ref. 17; whole-rock Pb–Pb and Rb–Sr respectively) representing three phases of activity. Singhbhum Granite Complex is exposed further southeast of the study area and comprises granitoids of different suites (tonalite/granodiorite, diorite and pegmatite) with intrusions of ultramafic suites and quartz veins (not shown in Figure 1*b*). A prominent N60°W–S60°E trending and 10–15 m wide polymictic conglomerate unit, with flattened and stretched pebbles of quartzite, quartz and chert within a siliceous (\pm sericite, \pm chlorite) matrix, is exposed intermittently in the southeastern extreme of the mapped area at the base of the SG (Figure 1*b*). Conformable trend of pebble lineations of the conglomerate and mineral stretching lineations in shear zone rocks seen in the above units suggests shear movement from NE towards the basement, as observed all along the SSZ. In the southeastern extreme of the study area, the conglomerates which mark the base of SG are underlain by grey quartzite and chlorite/biotite phyllite of the IOG. The phyllites are characterized by slaty cleavages trending N65°W–S65°E with a steep dip of 50–60° due N25°E. The quartzite is moderate to poorly sorted, composed of sub-rounded quartz grains and minor sericite, and is profusely traversed by silica veinlets. The phyllite and quartzite of the IOG have been intruded by peridotite. The peridotite contains caught-up patches of the IOG; therefore, is considered to be the late phase

of the IOG. It is completely serpentinized and exposed at 100–200 m south of Turamdih, where crude foliations along N50°W–S50°E to N55°W–S55°E with dip 35–40° due NE are preserved. The SG exposed to the north of this peridotite body, includes sericite chlorite quartz schist, chlorite quartz (\pm sericite) schist, sheared quartzite and quartz sericite schist with varying degrees of shearing and mylonitization. The chlorite quartz (\pm sericite) schist shows strong foliation trending N60°W–S60°E with dips 30°–40° due N30°E. Thus, the structural trends observed in the IOG, serpentinized peridotite and the SG are similar and correlated with the same event. In the main mineralized zone of the SSZ, uranium and copper are hosted in chlorite quartz schist where magnetite is an important by-product. The dominant minerals, viz. chlorite and quartz vary in proportion from 30% to 80% and 15% to 65% respectively, with respect to precursor lithounits. Sheared sericite quartzite occurring as bands within schist is a well-foliated arenaceous lithounit, where foliations are developed due to parallel arrangement of sericite and quartz. The quartz grains are elongated, often displaying ribbon-like texture. The foliation planes of quartzite preserve prominent development of intersection (stripping) and mineral stretching lineation, which are sub-parallel to each other. In addition, the feldspathic schists are intermittently exposed as a few scanty outcrops within soil-covered, cultivated land both east and west of Turamdih. These rocks do not show typical granitic texture; rather, they are a fine-grained, strongly foliated quartzo-feldspathic

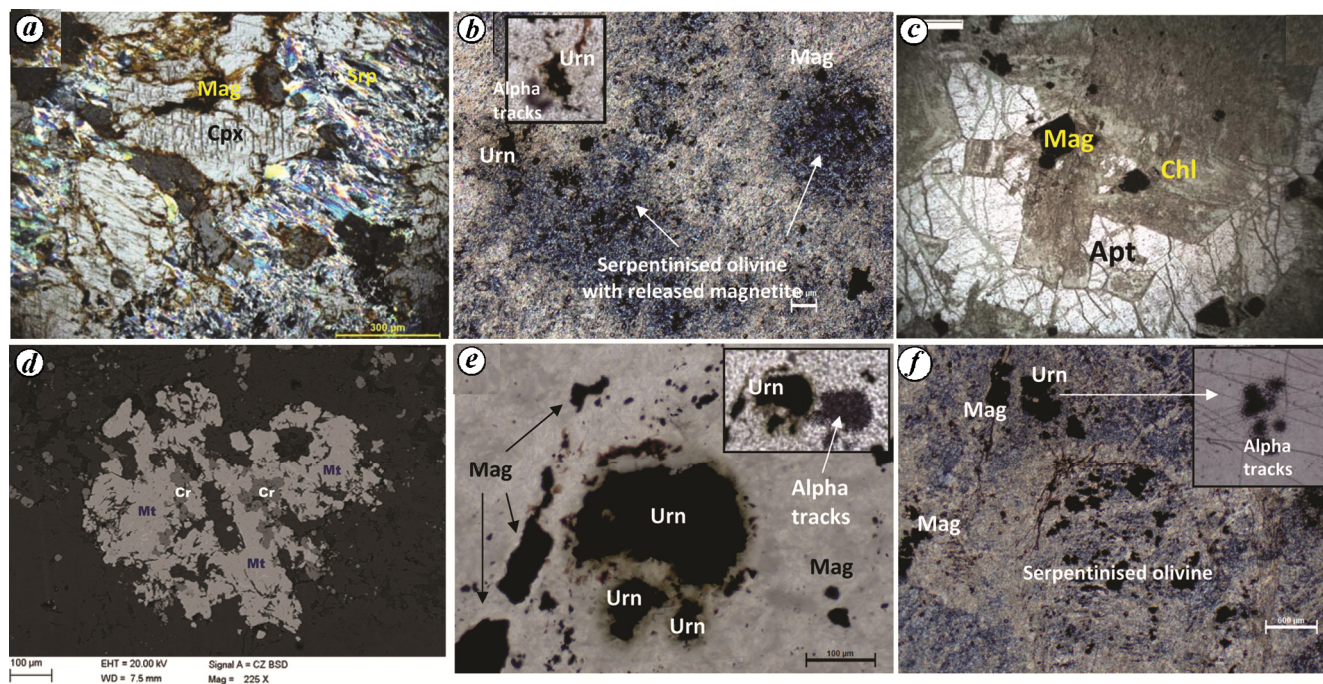


Figure 3. Photomicrographs showing petrography of host rock and mode of occurrence of uraninite. *a*, Relicts of clinopyroxenes in serpentinized peridotite outcrop, Kudada area. Transmitted light (TL), cross nicol (2N), 5× resolution (5×) in air. *b*, Uraninite and anhedral disseminated magnetite in association with serpentinized pseudomorphs after olivine with released magnetite at 442.15 m depth. TL, 2N, 2.5× in air. *c*, Euohedral apatite in association with euohedral magnetite and chlorite. Chlorite-filled fractures in apatite. TL, 2.5× in air. *d*, SEM image of chromite core within anhedral magnetite grain. 225×. *e*, Brownish radiation halo in serpentine surrounding uraninite grain. Associated magnetite showing no halo. At 442.15 m depth. (Inset) Dense alpha tracks of corresponding uraninite on cellulose nitrate (CN)-film on autoradiography. TL, 1N, 20× in air. *f*, Clusters of uraninite in association with magnetite and serpentinized olivine at 448.15 m depth. TL, 2N, 2.5× in air.

unit with varying proportions of albite, K-feldspar and quartz. Altered feldspar grains and sub-angular quartz grains alternating with sericite chlorite zones define the main schistosity in this lithounit. The feldspathic schist also trends in N60°W–S60°E to N50°W–S50°E with dips of 30–45° due N30°E and seen up to the foothills of Ramchandrapahar, north of Kudada. Small-scale north-westerly plunging, tight asymmetric folds are characteristic structural features observed in feldspathic schist.

Petrology of the host rock and uranium mineralization

The uranium mineralization occurs in serpentinized peridotite. The host is exposed as a narrow, 2 km long, E–W-trending ridge extending from Kudada in the west to Talsa village in the east, and falls within the limits of Kudada Reserve Forest (Figure 1 *b*). Megascopically, peridotite is a dark greenish-coloured, altered (serpentinized and chloritized) rock with disseminations and veins of magnetite (Figure 2 *a–d*). Patches of undigested IOG quartzite are mapped within the peridotite body, close to the uraniferous anomaly (0.035% U₃O₈; 0.005% ThO₂), which confirm that the peridotite is younger than the caught-up patches (Figures 1 *b*, 2 *e* and *f*). It is therefore a late phase of the IOG or even much younger than the entire IOG.

The host rock is dominantly composed of serpentine. Relicts of olivine, clinopyroxene, traces of pyrite, asbestos veinlets and magnetite of skeletal, disseminated and dusty variants are observed (Figure 3 *a*). The subsurface samples comprises dominantly of serpentine with relict pseudomorphs of olivine and clinopyroxene with minor proportion of talc, apatite and chlorite (chamosite). Rounded to sub-rounded as well as fairly tabular pseudomorphs of size varying from 3000 to 5000 μm after olivine and pyroxene respectively, are identified (Figure 3 *b*). Most of the pseudomorphs constituted by serpentine show fine disseminated exsolved opaques, while some of the pseudomorphs are rounded to oval-shaped, devoid of exsolved opaques. The latter probably represent altered pyroxene with olivine as inclusions. EMPA indicates that serpentine is Mg–Fe variety – antigorite type (Mg_{7.05}Ni_{0.01}Fe_{3.39}Mn_{0.03}Cr_{0.02})_{10.50}(Si_{7.75}Al_{0.19})_{7.94}O₂₀(OH)₁₆. This is actually a phase in the MgO–NiO–FeO–SiO₂–H₂O system. Chlorite is the alteration product after clinopyroxenes. Secondary veins of chlorite cutting across other phases have also been observed. Apatite occurs as euohedral to subhedral grains of size varying from 1 to 2 mm, often in chlorite-filled fractures (Figure 3 *c*). Occurrence of magnetite in varying textures and modes is evident in the host rock. The altered pseudomorphs of olivine consist of two textural varieties of magnetite: one with fine subhedral variant filling cracks and crevices, and the

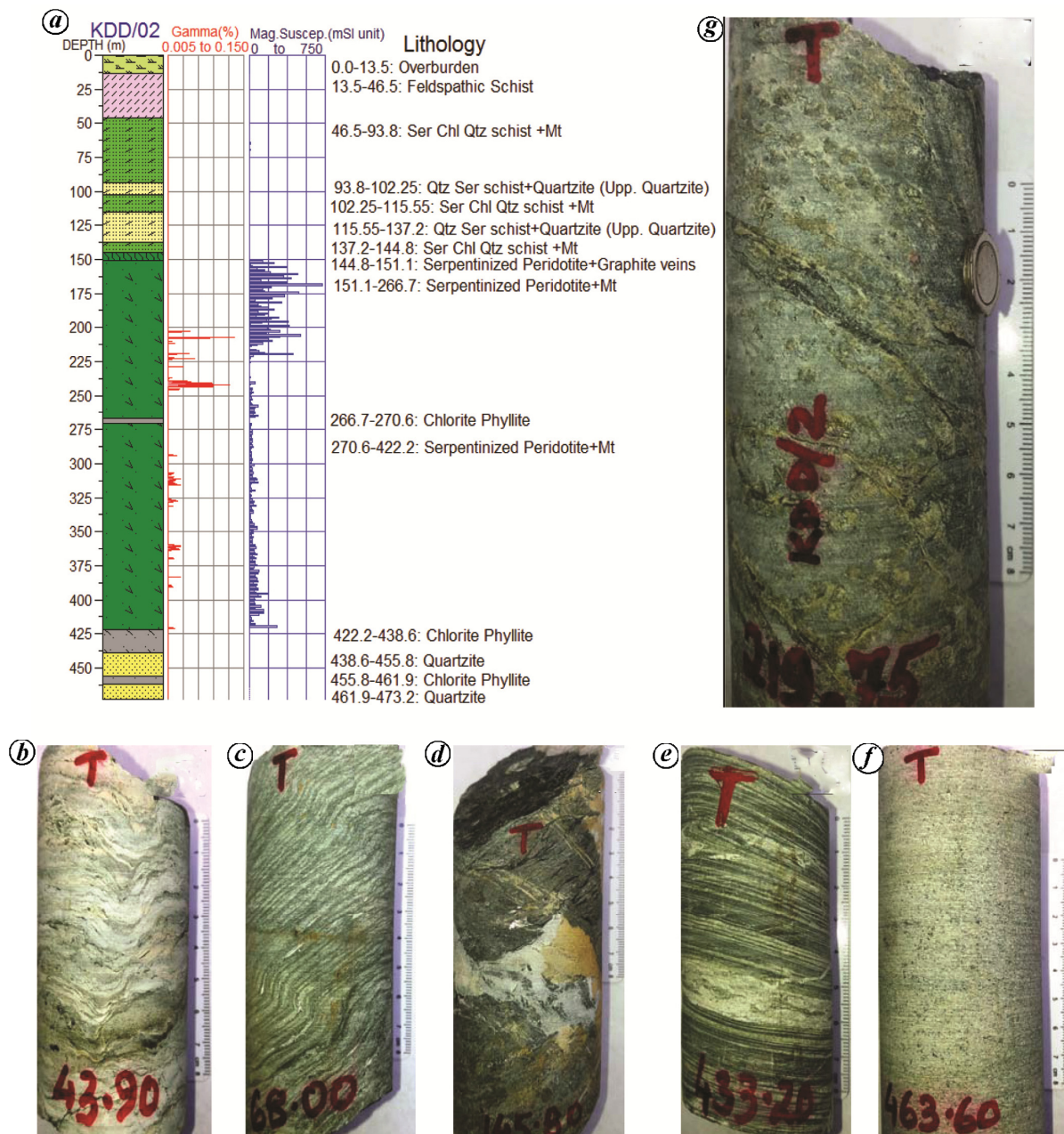


Figure 4. Borehole litholog, gamma ray, magnetic susceptibility log and representative core photographs of borehole KDD/2. Note high magnetic susceptibility corresponding to high gamma activity related to uranium. **a**, Borehole lithology showing comparison of gamma ray and magnetic susceptibility log. **b**, Feldspathic (\pm chlorite) schist of Singhbhum Group showing tight asymmetric folds at depth 43.90 m. **c**, Foliated chlorite quartz (\pm sericite) schist of Singhbhum Group showing S-shaped asymmetric folds at depth 68 m. **d**, Serpentinized peridotite of Iron Ore Group (IOG) with quartz and thin veins of graphite at depth 145.80 m. **e**, Chloritic phyllite (tuffaceous) with arenite bands of the IOG at depth 433.20 m. **f**, Arkosic quartzite (\pm sericite) of the IOG at depth 463.60 m. **g**, Uraniferous serpentinized peridotite with rounded to tabular grain relicts/pseudomorphs of olivine and pyroxene and thin chlorite veins at depth 219.75 m.

other dusty granules confined within the pseudomorphs. The crack-filling magnetites are restricted within the olivine pseudomorph and usually do not continue outside the same, which suggests that magnetite is released due to alteration of olivine to serpentine. Mesh texture defined by the serpentine mass and secondary magnetite derived from breakdown of olivine is preserved at places. Anhedra dissemminations of magnetite within the rock as sub-

hedral clots and as skeletal grains are also observed, which are interpreted as primary (?) magnetite. Magnetite is often present in association with maghemite, indicating its low temperature alteration.

SEM images of opaques showed core of chromite within some of the anhedra magnetite grains (Figure 3 d). Pyrite occurs as fine specks as well as veins, while chalcopyrite is mostly in the form of veins. XRD has

Table 1. Chemical analysis data of outcrops and borehole core of peridotite, Kudada area, Jharkhand, India

Sample code	Nature of sample	Elemental composition (%)														Elemental composition (ppm)										
		SiO ₂	TiO ₂	Al ₂ O ₃	Fe ₂ O ₃	FeO	MnO	MgO	CaO	K ₂ O	Na ₂ O	P ₂ O ₅	LOI	U ₃ O ₈	Th	Co	Cr	V	Cu	Ni	Mo	As	Au (ppb)	Pt (ppb)	CIA	Mg#
TRDU/1	Uraniferous	42.70	0.09	1.08	14.95	5.60	0.03	21.95	0.19	0.06	1.24	0.08	10.10	0.001	<10	79	1752	52	25	1347	10	50	<10	<10	32	67.24
TRDU/2		45.90	0.10	1.31	10.86	4.52	0.03	22.16	0.21	0.25	1.22	0.06	11.70	0.001	<10	65	1939	68	<10	1092	<10	15	<10	<10	34	73.42
TRDU/3		46.50	0.08	1.10	11.49	3.61	0.03	22.25	0.14	0.09	1.22	0.03	12.00	0.001	<10	63	1907	67	<10	1121	<10	<10	<10	<10	32	73.97
TRDU/4		36.10	0.10	1.71	23.66	4.70	0.03	20.21	0.46	0.59	1.27	0.21	9.47	<0.001	<10	43	1468	36	10	895	10	45	<10	<10	36	58.08
KUD/16	Uraniferous	33.46	0.11	1.10	12.25	6.21	0.02	26.0	1.12	0.03	0.62	0.62	17.33	0.014	<10	168	295	230	52	3570	18	NA	NA	NA	41	72.89
KUD/19		33.49	0.10	1.00	13.58	6.39	0.02	25.7	0.43	0.03	0.55	0.25	17.27	0.030	<10	633	493	230	90	9530	16	NA	NA	NA	47	71.1
KUD/23		33.00	0.12	0.94	12.42	6.03	0.01	26.1	1.01	0.08	0.41	0.20	17.93	0.019	<10	410	340	230	69	7140	12	NA	NA	NA	50	72.99
KUD/24		33.20	0.07	0.82	12.88	6.39	0.01	26.6	0.31	0.02	0.37	0.17	17.89	0.025	<10	589	350	205	93	9060	30	NA	NA	NA	51	72.5
TRDU/14 416.80	Uraniferous borehole core	41.73	0.10	1.17	5.50	14.60	0.16	25.97	1.65	0.06	0.60	0.66	5.98	0.002	<10	38	2363	173	44	327	50	NA	NA	NA	32	70.29
TRDU/14/ 438.05		41.74	0.10	1.18	4.07	12.40	0.12	25.43	4.10	0.05	0.66	2.21	5.96	0.006	<10	34	2130	70	37	222	21	NA	NA	NA	20	76.89
TRDU/ 14/482.75		41.69	0.08	1.13	2.39	11.20	0.12	24.98	6.59	0.08	0.71	3.69	5.79	0.009	10	39	2856	70	58	318	29	NA	NA	NA	51	74.84
TRDU/14 494.50m		44.35	0.14	1.33	2.51	14.50	0.19	27.93	0.19	0.17	0.55	0.07	6.24	<0.001	<10	39	2856	70	58	318	29	NA	NA	NA	51	74.84
TRDU/14 441.5m	Uraniferous borehole core	45.20	0.06	1.18	9.90	7.95	0.10	19.23	3.86	0.06	1.07	2.84	6.00	0.188	<10	157	1623	85	178	502	292	195	30	<10	36	67.02
TRDU/14 442.15m		46.70	0.07	1.18	10.69	9.21	0.11	19.71	1.52	0.06	0.98	1.21	6.21	0.055	<10	273	1913	107	37	777	485	590	26	<10	43	65.10
TRDU/14 448.15m		37.30	0.10	1.31	5.89	17.30	0.12	18.39	4.62	0.06	0.96	4.09	6.00	0.123	<10	158	3165	191	19	671	286	755	11	47	84	59.14
TRDU/14 473.75m		50.60	0.07	1.30	2.43	13.60	0.15	20.17	0.65	0.15	1.06	0.43	6.82	0.031	<10	43	1823	87	170	297	85	<10	<10	<10	95	69.55
TRDU/14 517m	45.70	0.06	1.15	2.52	13.40	0.18	20.89	1.40	0.05	1.09	0.98	9.74	0.117	<10	63	1873	46	17	575	14	35	<10	<10	36	70.43	
Sample code	Nature of sample	La	Ce	Pr	Nd	Sm	Eu	Gd	Tb	Dy	Ho	Er	Tm	Yb	Lu	Sc	Y	Total REE	(La/Lu) ^{CN}	Gd/Yb ^{CN}	La/Sm ^{CN}	Eu/Eu ^{*CN}				
TRDU/14 416.80m	Uraniferous borehole core	40	96	10	41	9	<2	5	<2	<5	<5	<5	<2	<5	<2	12	22	235	-	-	2.87	-				
TRDU/14 438.05m		39	87	<10	38	8	<2	<5	<5	<5	<5	<5	<2	<5	<2	8	52	232	-	-	3.15	-				
TRDU/14 494.50m		7	20	<10	9	<5	<2	<5	<5	<5	<5	<5	<2	<5	<2	8	14	58	-	-	-	-				
TRDU/14 441.5m		506	985	100	417	90	2	76	10	32	5	10	1	10	1	2	5	125	2376	27.11	6.29	3.63	0.07			
TRDU/14 442.15m	Uraniferous borehole core	250	492	50	210	45	1	35	4	14	3	5	1	6	1	7	80	1204	26.79	4.83	3.59	0.07				
TRDU/14 448.15m		810	1510	150	620	130	4	90	12	36	6	10	1	10	3	7	137	3536	28.94	7.45	4.02	0.11				
TRDU/14 473.75m		20	46	<10	27	11	<1	20	<2	<5	<2	<2	<1	<2	<1	8	55	187	-	-	1.17	-				
TRDU/14 517m		85	169	17	70	16	1	15	2	10	<2	5	<1	6	<1	7	86	489	-	-	3.43	0.19				

CN, Chondrite normalizing values after sun and McDonough, 1989.

confirmed the presence of other ore minerals, viz. cobaltite (CoAsS), cerussite (PbCO₃), nickeline (NiAs), vaesite (NiS₂), molybdenite, and traces of monazite and beta uranophane. Apart from these, presence of a variety of carbonates like calcite, dolomite and siderite in the host rock suggests that there was an influx of CO₂ to the system.

Uranium mineralization in serpentized host rock has been disseminated heterogeneously. The grains are pitted in appearance and show distinct brownish radiation haloes around them as well as dense alpha tracks on the CN-film subsequent to autoradiography (Figure 3e). Size of these grains ranges from 10 to 600 µm. Clustering of uraninite, where at least three grains have grown together, has been observed (Figure 3f). Magnetite of varying sizes ranging from dusty fine grains to as large as 500 µm is found in the vicinity of uraninite. Specks of galena are observed within micropits of uraninite. Unit cell dimension of uraninite ranges from 5.4498 Å to 5.4650 Å, which matches well with the values reported from the SSZ and is indicative of high temperature (300–500°C) of crystallization. Stoichiometric deviation of oxygen contents in the formulae unit varies from UO_{2.187} to UO_{2.046}.

Subsurface continuity of uranium mineralization

The present phase of exploration in the Turamdih–Kudada block is confined to probe lateral continuity and depth persistence of the uraniferous serpentized peridotite body. The borehole TRDU/14, drilled north of Turamdih, intercepted mineralized peridotite body and confirmed its depth persistence. The continuity has been further established in subsequent boreholes TRDU/15 and TRDU/16 drilled to the updip and downdip of TRDU/14 respectively (Figure 1b). The boreholes drilled through the cover of SG have proved the depth continuity of serpentized peridotite-hosted moderate to high-grade uraniferous lodes (0.001–0.188% U₃O₈; Table 1). It confirmed a new type of uranium mineralization in an unusual host rock¹⁸. Subsequent boreholes have further proved ~300 m thickness of the peridotite body below the SG (Figure 4a–c) and recorded continuity of mineralization with similar characters. The graphitic matter has been observed along the partings/fractures at the hang-wall side of the peridotite (Figure 4d). In a few boreholes, thin (<5 m), intermittent, non-magnetic, chlorite phyllite, biotite phyllite and slate units of the IOG with oblique fractures and smooth, polished fracture plane/core partings have been recorded within the peridotite. This shows the undigested part of the IOG phyllites (Figure 4e). Arkosic quartzites (± sericite) of the IOG mark the footwall contact of the intrusive peridotite in the boreholes (Figure 4f). The borehole core from the mineralized peridotite zone is characterized by rounded to

tabular grain relics of olivine and pyroxene along with thin chlorite veins (Figure 4g). Comparison of borehole lithology, gamma ray and magnetic susceptibility indicates that magnetite veins/disseminations in the serpentized peridotite account for the highest order of magnetic susceptibility (av. 170 nT; *n* = 44). Exploratory drilling in Turamdih–Kudada area has so far established about 1 km downdip continuity and 600 m strike continuity of the mineralized peridotite, which is open for further exploration.

Geochemistry of peridotite

The outcrop and core samples from peridotites (*n* = 17) have high MgO (18–28%), Fe₂O₃ (2–24%), FeO (4–17%), CaO (0.14–4.62%), P₂O₅ (0.03–4.09%), Cr (295–3165 ppm), Ni (222–9530 ppm), Mo (<10–485 ppm), Co (34–633 ppm), V (36–230 ppm), Cu (<10–173 ppm) and low SiO₂ (33%–50%), TiO₂ (0.06%–0.14%), Al₂O₃ (0.94%–1.71%), K₂O (0.02–0.59%), Na₂O (0.37–1.27%) and ThO₂ (<10 ppm). Loss on ignition (LOI) varies from 6% to 18%, which is due to the presence of carbon and water-bearing phases as mentioned earlier in the text (Table 1).

The uraniferous samples (>0.010% U₃O₈) are distinctively different from the non-mineralized (<0.010% U₃O₈) suite in having higher U, CaO, P₂O₅, Co, Ni, V, Cu and Mo content (Table 1). Chemical index of alteration (CIA) shows variation in the degree of alteration in mineralized and non-mineralized peridotite based on selective removal of labile cations like Ca²⁺, Na⁺, K⁺ relative to stable residual constituents like Al³⁺ and Ti⁴⁺ (ref. 19). Values are overlapping in certain cases; but in general, uranium mineralized peridotite (av. 48) is comparatively more altered than its non-mineralized (av. 33) counterpart. This suggests that alkalis have been removed from the ore zone of peridotite. The IUGS classification of high-Mg volcanic rocks²⁰, groups the studied rock (MgO >18%, SiO₂ < 52%, TiO₂ < 1% and total alkali, i.e. Na₂O + K₂O < 2%) as komatiite²¹. The total alkali versus silica binary plot²⁰ and CaO–MgO–Al₂O₃ ternary plot²² suggest komatiitic nature of peridotite (Figure 5a and b). Moreover, core samples have shown the presence of Au (<10–30 ppb, *n* = 5), Pt (<10–95 ppb; *n* = 5) and As (<10–755 ppm; *n* = 5) in accordance with their komatiitic parentage. The uraniferous peridotite samples from the core have analysed higher total REE (av. 1558 ppm; *n* = 5) compared to the non-mineralized peridotite core (av. 175 ppm; *n* = 3). Worldwide reported komatiites generally show a flat REE pattern along with low REE content. The REE pattern with negative Eu anomaly and LREE > HREE content in uraniferous sample is attributed to the presence of apatite. This is also corroborated with strong positive correlation of CaO (*r* = 0.65) and P₂O₅ (*r* = 0.86) with total REE. Fractionation among

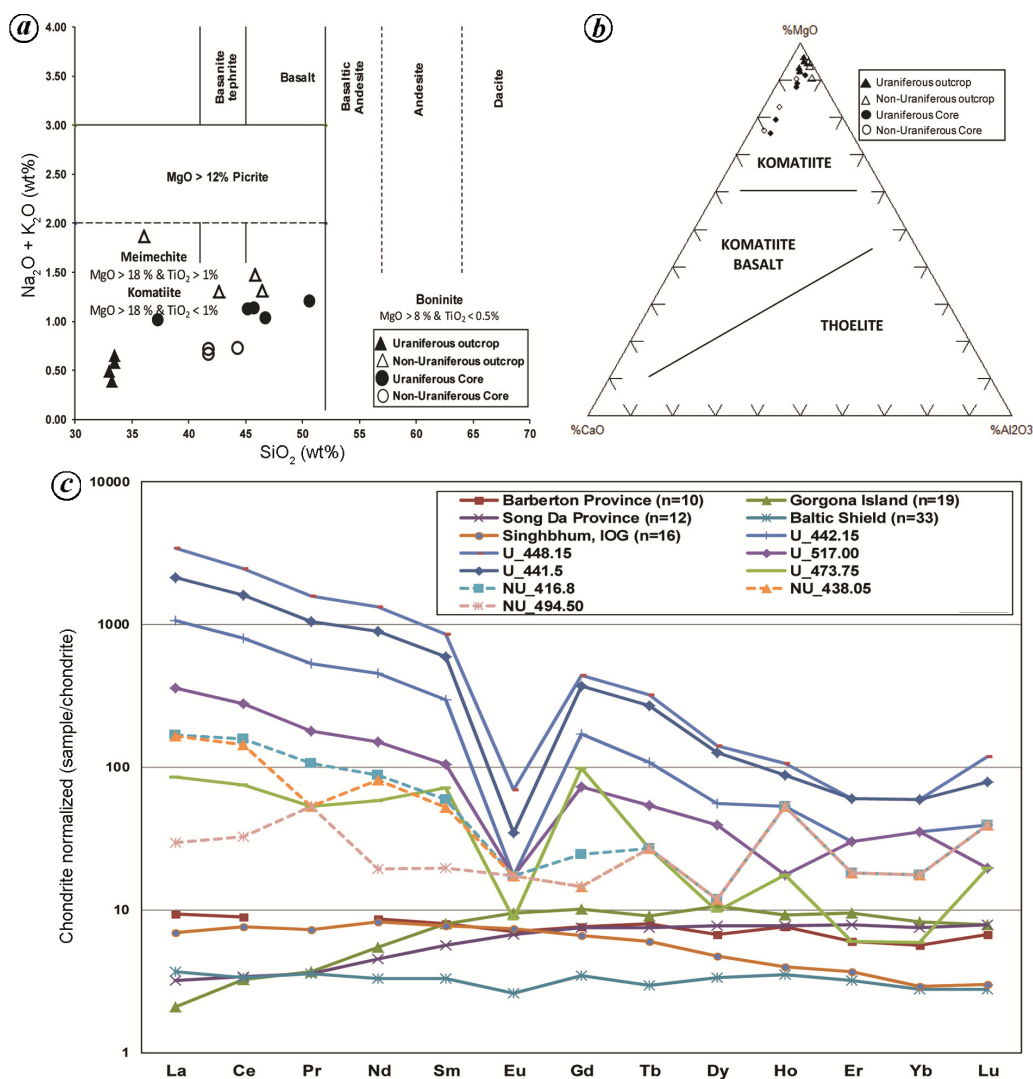


Figure 5. *a*, Total alkali–silica plot showing komatiitic nature of peridotite (after Le Bas²⁰). *b*, CaO–MgO–Al₂O₃ ternary plot showing komatiitic nature of peridotite (after Viljoen *et al.*²²). *c*, Chondrite normalized REE plot for uraniferous (continuous lines), non-mineralized core (dotted lines) shown with respect to worldwide reported komatiites (normalizing values after Sun and McDonough²³).

LREE is distinct in uraniferous core samples, which is corroborated by the $\text{La}/\text{Sm}_{(\text{CN})}$ and $\text{La}/\text{Sm}_{(\text{PM})}$ ratios (1.17–4.03). A strong negative Eu anomaly is characteristic of the chondrite normalized REE plot of uraniferous serpentinized peridotites (Figure 5c)²³. Apatite generally shows discrimination against Eu in its lattice and thus accounts for negative Eu anomaly²⁴.

Discussion and conclusion

Discovery of medium-grade uranium mineralization along with significant Cr–Ni–Mo–REE–Fe–Mg elements in serpentinized peridotite on the surface as well as in boreholes, opens up the possibility of unearthing a unique polymetallic deposit in the environs of the SSZ. The SSZ domain, which was earlier known for uranium (\pm Cu, Fe) deposits in the SG, now has another potential host. The peridotite-hosted uranium mineralization in Kudada area

therefore provides an opportunity to develop a novel exploration model in the Singhbhum domain¹⁷. Peridotite is interpreted as the last phase of the IOG. Its intrusive relationship has provided a lithostructural guide for uranium exploration.

Serpentinization of rocks requires generation and maintenance of transport pathways for water. The solid volume increase during serpentinization can lead to stress build-up and trigger cracking, which ease fluid penetration into the rock. Considering the above ideas, it is suggested that fluid-driven hydrothermal alteration led to widespread serpentinization of the host peridotite. This witnessed concurrent epigenetic hydrothermal uranium mineralization. The hydrothermal activity related to uranium mineralization is confined along certain weak planes in the central part of the peridotite body, and accordingly, as we move towards the footwall or hang-wall side, the grade of uranium mineralization leans out.

CIA values indicate that alteration is also relatively more intense in the mineralized zones. Dissemination of magnetite as subhedral clusters as well as skeletal grains is the primary magnetite (Mt-1). The serpentinization has released microcrack-filling magnetite (Mt-2) in olivine pseudomorphs, dusty magnetite (Mt-3) within chamosite, while the veins of magnetite (Mt-4) suggest that they have been introduced later along with metallogenesis of uranium.

This polymetallic (U–Cr–Ni–Mo–REE–Fe–Mg) mineralization in comparison with the well-known SSZ-related uranium mineralization is a subject matter of new research. Syngenetic Cr–Ni–Mo–Fe–Mg concentration in komatiite is acceptable, but uranium and REE concentrations need to be accounted by the epigenetic process. Komatiite has attracted uranium mineralization because of its mafic nature, where FeO might have contributed to the reduction of uranium. Syngenetic concentration of Cr–Ni–Mo–Fe–Mg, and epigenetic U and REE have raised the overall tenor in an unusual geological environment. The host rock in the present case belongs to the IOG, and mineralization may be synchronous to the SSZ uranium mineralization. Unit cell dimension of uraninite (5.4498–5.4650 Å) in serpentinized peridotite is comparable with the values reported from other uranium deposits of the SSZ, which is indicative of high temperature (300–500°C) crystallization of uraninite. In this background, epigenetic hydrothermal process of formation, akin to SSZ type of uranium mineralization is proposed for the serpentinized peridotite-hosted mineralization in Kudada area.

The peridotite-hosted uranium mineralization has not been reported earlier from the SSZ. Although several aspects of this prospective polymetallic mineralization and the host rock are discussed here, there is ample scope for further research related to genetic aspects of mineralization in this unusual host rock.

- Dunn, J. A., The geology of North Singhbhum including parts of Ranchi and Manbhum Districts. *Mem. Geol. Surv. India*, 1929, **54**, 166.
- Dunn, J. A. and Dey, A. K., Geology and petrology of Eastern Singhbhum and surrounding areas. *Mem. Geol. Surv. India*, 1942, **69**(2), 281–456.
- Rao, N. K. and Rao, G. V. U., Uranium mineralization in Singhbhum Shear Zone, Bihar. I. Ore mineralogy and petrography. *J. Geol. Soc. India*, 1983, **24**, 437–454.
- Sarkar, S. C., Uranium (–nickel–cobalt–molybdenum) mineralization along the Singhbhum copper belt, India, and the problem of ore genesis. *Miner. Deposita*, 1982, **17**(2), 257–278.
- Pal, D. C. and Rhede, D., Geochemistry and chemical dating of uraninite in the Jaduguda uranium deposit, Singhbhum Shear Zone, India – implications for uranium mineralization and geochemical evolution of uraninite. *Econ. Geol.*, 2013, **108**(6), 1499–1515.
- Sinha, K. K., Das, A. K., Sinha, R. M., Upadhyay, L. D., Pandey, P. and Shah, V. L., Uranium and associated copper nickel molybdenum mineralization in Singhbhum Shear Zone, Bihar, India: present status and exploration strategy. *EARFAM*, 1990, **3**, 27–43.
- Mahadevan, T. M., In *Geology of Bihar and Jharkhand*, Text Book Series, Geological Society of India, Bangalore, 2000.
- Pandey, P., Kumar, P. and Upadhyay, L. D., Uranium deposits of Turamdih–Nandup area, Singhbhum district, Bihar and their spatial relationship. *EARFAM*, 1994, **7**, 1–13.
- Saha, A. K., Crustal evolution of Singhbhum, North Orissa, Eastern India. *Mem. Geol. Soc. India*, 1994, **27**, 341.
- Chaudhuri, T., Wan, Y., Mazumder, R., Mingzhu, M. and Liu, D., Evidence of enriched, Hadean mantle reservoir from 4.2–4.0 Ga zircon xenocrysts from Paleoproterozoic TTGs of the Singhbhum Craton, Eastern India. *Nature, Sci. Rep.*, 2018, Article 7069, doi:10.1038/s41598-018-25494-6.
- Mukhopadhyaya, D., The Archaean nucleus of Singhbhum: the present state of knowledge. *Gondwana Res.*, 2001, **4**, 307–318.
- Gupta, A. and Basu, A., North Singhbhum Proterozoic mobile belt Eastern India – a review. *Geol. Surv. India, Spec. Publ.*, 2000, **55**, 195–226.
- Acharyya, S. K., A plate tectonic model for Proterozoic Crustal evolution of Central Indian Tectonic Zone. *Gondwana Geol. Mag.*, 2003, **7**, 9–31.
- Mazumder, R., Eriksson, P. G., De, S., Bumby, A. J. and Lenhardt, N., Palaeoproterozoic sedimentation on the Singhbhum Craton: global context and comparison with Kaapvaal. *Geol. Soc., London, Spec. Publ.*, 2012, **365**, 49–74; <http://dx.doi.org/10.1144/SP365.4>.
- Banerji, A. K., Ore genesis and its relationship to volcanism, tectonism, granitic activity and metasomatism along the Singhbhum Shear Zone, Eastern India. *Econ. Geol.*, 1981, **76**, 905–912.
- Sarkar, S. C., Geology and ore mineralisation along the Singhbhum copper uranium belt, Eastern India. Jadavpur University, Calcutta, 1984, p. 263.
- Sarkar, S. N., Ghosh, D., Lambert, R. J., Rb–Sr and lead isotopic studies on the soda granites from Mosaboni, Singhbhum Copper Belt, Eastern India. *J. Earth Sci.*, 1986, **13**, 101–116.
- Sinha, D. K. and Verma, M. B., The uranium potential in the Singhbhum Shear Zone: future prospects. International Symposium by International Atomic Energy Agency, Extended Abstract, 2018, pp. 393–398.
- Nesbitt, H. W. and Young, G. M., Early Proterozoic climate and plate motions inferred from major element chemistry of lutiites. *Nature*, 1982, **299**, 715–717.
- Le Bas, M. J., IUGS Re classification of the high Mg and picritic volcanic rocks. *J. Petrol.*, 2000, **41**(10), 1467–1470.
- Viljoen, M. J. and Viljoen, R. P., The geology and geochemistry of the lower ultramafic unit of the Onverwacht Group and a proposed new class of igneous rocks. *Geol. Soc. S. Afr. Spec. Publ.*, 1969, **2**, 55–86.
- Viljoen, M. J., Viljoen, R. P. and Pearton, T. N., The nature and distribution of Archaean komatiite volcanics in South Africa (eds Arndt, N. T. and Nisbet, E. G.), Allen and Unwin, London, 1982, pp. 53–79.
- Sun, S. S. and McDonough, W. F., Chemical and isotopic systematics of oceanic basalts: implications for mantle composition and processes. *Geol. Soc. London, Spec. Publ.*, 1989, **42**, 313–345.
- Eby, G. N., Abundance and distribution of the rare-earth elements and yttrium in the rocks and minerals of the Oka carbonatite complex, Quebec. *Geochim. Cosmochim. Acta*, 1975, **39**, 597–620.

ACKNOWLEDGEMENT. We thank our colleagues in the physics, chemistry, XRF, XRD, EPMA laboratories for analytical support.

Received 1 November 2018; revised accepted 29 May 2019

doi: 10.18520/cs/v117/i5/830-838